ADVANCED MATERIALS
www.advmat.de

Centrifugal Shape Sorting and Optical Response of Polyhedral Gold Nanoparticles

*Yu Jin Shin, Emilie Ringe, Michelle L. Personick, M. Fernanda Cardinal, Chad A. Mirkin, Laurence D. Marks, Richard P. Van Duyne, and Mark C. Hersam**

Metallic nanostructures are of high interest because their optical properties can be tuned throughout the visible and near-infrared portions of the electromagnetic spectrum by adjusting nanoparticle shape, size, composition, and local dielectric environment.[1–4] In particular, the localized surface plasmon resonance (LSPR) properties of metal nanoparticles have shown promising applications in chemical and biological sensing,[5–7] waveguiding,[8] single-particle tracking,[9] and surface enhanced Raman spectroscopy (SERS).[10,11]

Since inhomogeneous broadening resulting from nanoparticle size and shape variations causes an increase in the linewidth of bulk LSPR spectra, monodispersity of the nanoparticle population is critical for optimal performance in LSPR-based devices and sensors.[12] Towards that end, previous studies have focused on obtaining more homogeneous nanoparticle populations by means of post-synthetic separation techniques, including size exclusion chromatography,[13] gel electrophoresis,[14] and centrifugation.[15] Among these methods, density gradient centrifugation has proven to be particularly successful, resulting in narrow distributions of gold nanoparticle diameters,[16] shapes,[17] and aggregation state.[18] Recently, Akbulut et al.[19] reported the use of aqueous multiphase systems as media for rate-zonal centrifugation to separate the reaction products (i.e., nanorods, nanospheres, and large particles) of a nominal gold nanorod synthesis, ultimately increasing the nanorod purity from 48% to 99%.

The shape-dependent optical properties of metal nanostructures have also motivated efforts to realize new nanoparticle shapes via novel synthetic routes[20–29] and to correlate nanoparticle structure with plasmonic behavior.[21,30–33] Among available nanoparticle shapes, gold bipyramids (BPs) are of interest because of their sharp tips, which lead to strong localized field enhancement and high sensitivity to the surrounding dielectric environment.[34–37] In particular, {110}-faceted gold BPs consisting of two triangular pyramids joined by a (111) twin plane have shown high stability and resistance to oxidative etching compared to other structures with near-infrared resonances.[38] Despite the potential of small BPs (i.e., BPs with edge lengths in the sub-100 nm range that show LSPR at visible wavelengths), relatively few reports[34,39] have studied their optical properties, owing to their relatively low synthetic yields. Indeed, current synthetic approaches produce only ca. 30% BPs, although in the specific case of {711}-faceted penta-twinned gold BPs (50 nm in length), BPs have been isolated at the >90% purity level by electrolyte-induced electrostatic screening.[40]

In this Communication, we describe a reliable and effective strategy for separating sub-100 nm, {110}-faceted gold nanostructures (i.e., rhombic dodecahedra (RD) and triangular BPs). By centrifuging the as-synthesized, unsorted mixture in a shallow iodixanol density gradient, we have isolated highly enriched solutions of BPs and RD as verified by scanning electron microscopy (SEM) and optical spectroscopy. Owing to the strong local field enhancement from the sharp tips of the BPs, the sorted BP sample provides refractive index sensitivity 2.5 times that of the as-synthesized, unsorted mixture. These ensemble measurements are further corroborated by single-particle LSPR spectra with the distribution of the plasmon resonance energies of the sorted particles quantified by means of dark-field optical microscopy.

As-synthesized, unsorted mixtures of {110}-faceted RD and triangular BPs were obtained through a Ag-assisted, seed-mediated growth method as detailed in the Supporting Information.[38] When the BPs are large (edge length > 200 nm), they can be separated from the much smaller RD using a commercial syringe filter.[38] However, for smaller BPs with plasmon resonances in the visible range that are synthesized through the addition of a higher concentration of seed particles, separation becomes challenging for three reasons: 1) small BPs easily pass through the 200 nm filter pores of commercial filters; 2) the size difference between BPs and RD decreases; 3) strong van der Waals interactions between the nanoparticles and filters with pore size < 200 nm render their removal difficult or impossible.

Since the aforementioned issues can be traced back to the limitations of filtration methods for small nanoparticle separations, we sought a centrifugation approach that eliminated the need for filters. In particular, a highly concentrated, as-synthesized gold nanoparticle (AuNP) solution (**Figure 1** A) was loaded onto the density gradient medium iodixanol, which was selected because its high viscosity slows the sedimentation of AuNPs to the point where subtle differences can be exploited

Y. J. Shin, Prof. L. D. Marks, Prof. M. C. Hersam
Department of Materials Science and Engineering
Northwestern University
Evanston, IL 60208, USA
E-mail: m-hersam@northwestern.edu
Dr. E. Ringe, Prof. R. P. Van Duyne
Department of Materials Science and Metallurgy
Pembroke Street, Cambridge, CB2 3QZ, UK
M. L. Personick, Dr. M. F. Cardinal, Prof. C. A. Mirkin
Department of Chemistry
Northwestern University
Evanston, IL 60208, USA

DOI: 10.1002/adma.201301278

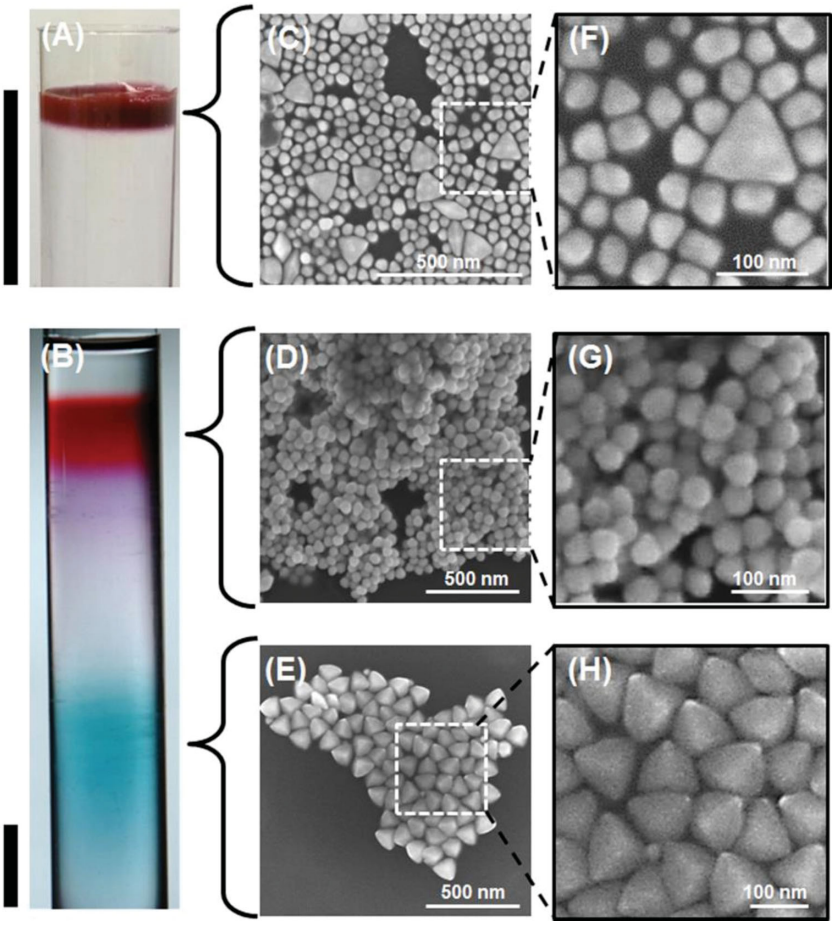

Figure 1. Photographs of a centrifuge tube before (A) and after (B) centrifugation of a concentrated AuNP solution in a shallow linear density gradient. C–E) Corresponding SEM images of the as-synthesized, unsorted sample (C), sorted RD (D), and sorted BPs (E). Magnified images are shown in the right-hand column (F–H). The vertical, black scale bars in (A) and (B) represent 1 cm.

for sorting. In this case, the difference in size between the RD and BP AuNPs leads to the expectation that the BPs should sediment more quickly than RD, although other factors such as nanoparticle shape and surfactant loading could also play a role.[17,18] In particular, the sedimentation coefficient is given by $S = m_p(1 - \rho_{m/}\rho_{p)}/f$, where m_p is the mass of the particle, ρ_p the density of the particle, ρ_m the density of the medium, and f the frictional coefficient. Hubbard and Douglas[41] previously reported the frictional coefficient of various Brownian particles. In our case, a BP can be treated as a tetrahedral dimer, whereas RD can be approximated as spheres owing to its highly faceted structure, ultimately implying a ~20% difference in f. However, the mass of BPs is 2.4 times that of RD, owing to the nanoparticle size difference (approximate edge lengths of BP and RD are 85 nm and 25 nm, respectively). Therefore, the mass difference is significantly greater than the frictional coefficient difference, and thus should be the primary factor in the resulting centrifugal separation.

To test this hypothesis, the shallow density gradient was centrifuged at 2 krpm for 60 min using a Beckman SW41Ti rotor, after which two distinct bands of AuNPs were observed (Figure 1B) and fractionated at a resolution of 1 mm. SEM images of the unsorted, sorted RD, and sorted BP samples are shown in Figures 1C–E. The blue (bottom) and dark pink (top) bands correspond to BPs and RD, respectively. As RD are the dominant reaction product, the color of the as-synthesized, unsorted solution resembles that of the RD fraction, although sorting reveals the presence of BP nanoparticles with strikingly different optical properties.

These optical properties were studied by extinction (UV-vis-NIR) spectroscopy as shown in **Figure 2**. Specifically, the normalized extinction spectra of unsorted, sorted RD, and sorted BP fractions are reported in Figure 2A. Only one peak, around 533 nm, was visible in the unsorted sample because of the overwhelming majority of RD, leading to the near-perfect match between the resonance peak position in the spectrum of the unsorted mixture and the sorted RD sample. However, the broader size distribution in the unsorted solution causes a wider resonance peak, as expected from heterogeneous broadening. The other fractions, consisting of sorted BPs, display intense extinction spectra with a main peak centered around 640 nm and a secondary peak at 533 nm that can be attributed to the predominant BPs and residual RD, respectively. The full evolution of the optical properties of the sorted fractions is shown in Figure 2B. As the collected fraction progresses to the lower part of the centrifuge tube (i.e., from fraction 10 to fraction 50), the relative intensity of the RD band (~533 nm wavelength) gradually decreases, while the red resonance of the BPs increases.

In addition to this optical evidence for separation, the nanoparticle population for each sample was quantitatively determined by counting a large number of nanoparticles ($N = 800$) in SEM images (Figure 2C). This SEM analysis reveals that the unsorted mixture consists of fewer than 20% BPs with the remainder being RD and a small amount of other shapes. In the sorted samples, the dark pink band contains exclusively RD (100%) whereas the blue band consists of more than 80% BPs with the remainder being residual RD and other shapes such as penta-twinned particles.

To evaluate the utility of the sorted BP solutions, refractive index sensitivity (RIS) measurements were performed. Glycerol/water mixtures were chosen as the tunable refractive index medium because of their compatibility with cationic surfactant-stabilized AuNPs.[39] **Figure 3** shows a plot of the LSPR peak wavelength as a function of the solution refractive index for the unsorted, sorted RD, and sorted BP samples (see Figure S1 and Table S1 in the Supporting Information for the raw and Gaussian-fitted UV-vis-NIR absorption spectra and resonance peak position of each sample under different conditions). The experimental data show a well-behaved linear dependence,

Adv. Mater. **2013**,
DOI: 10.1002/adma.201301278

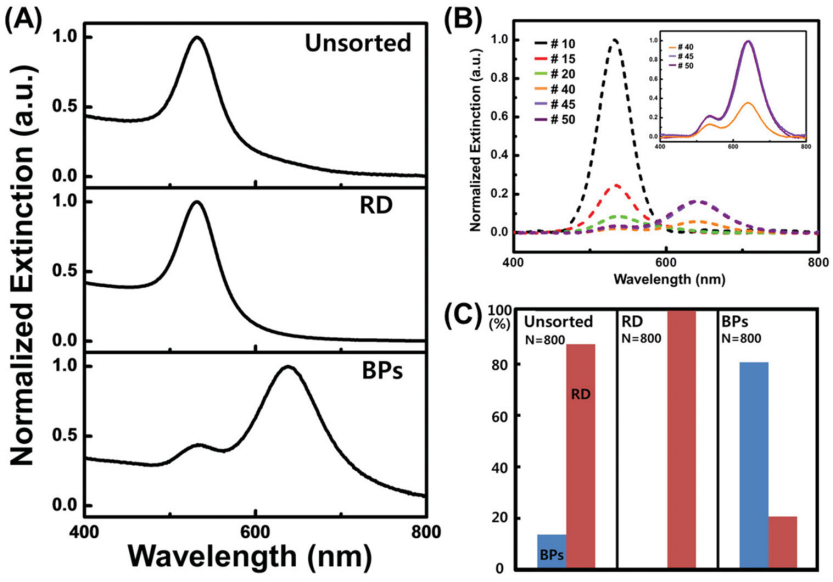

Figure 2. A) Normalized extinction spectra for the unsorted, sorted RD, and sorted BP samples. B) The evolution of the surface plasmon resonance of sorted AuNPs from the top to the bottom band following density gradient centrifugation. The inset shows normalized magnified spectra of the BP fractions. C) Corresponding population histograms determined from SEM (N = 800 AuNPs were counted for each histogram).

thus allowing the RIS to be directly extracted from the slope of the linear fits. The unsorted sample, which contains predominantly RD, has a RIS of 66 nm/RIU (where RIU is refractive index unit). This value is slightly higher than that of the sorted RD (56 nm/RIU) owing to the small amount of BP in the unsorted sample. In contrast, for the sorted BP solution, the RIS increases substantially to 170 nm/RIU, which is 2.5 times that of the as-synthesized, unsorted sample. This result corresponds well with previous findings on similar particles (150 nm/RIU),[39] but more importantly it demonstrates the major improvement in sensitivity that can be obtained by means of density gradient centrifugation. It should also be noted that this RIS enhancement was reproducible for multiple batches of sorted AuNPs, thereby demonstrating the ability of this separation method to reliably overcome batch-to-batch variations in synthesis. In addition to RIS, the refractive index figure of merit (FOM) is defined as the ratio of RIU to the full width at half maximum (FWHM) of the spectra and is also shown in Table S2 (Supporting Information). Furthermore, dynamic light scattering of the particles in a 75% glycerol/water mixture confirms colloidal stability, thus verifying that the resonance peak shift is not an effect of nanoparticle aggregation (see Figure S2 and Table S3, Supporting Information).

In order to study subtle differences between closely spaced fractions, single-particle analysis was performed using dark-field microscopy, a technique in which only the scattered light from the particles is collected and recorded on a charge-coupled device (CCD) camera, as described previously.[31,33,42,43] Results from fitting Lorentzian lineshapes to single-particle spectra from three different fractions of the same synthesis batch are reported in **Figure 4**. Fraction 12 consists of RD, while fractions 24 and 27 contain mostly BPs, as shown in SEM images (Supporting Information, Figure S3). These cetyltrimethylammonium chloride (CTAC)-capped AuNPs sustain strong plasmon resonances, as previously noted.[38] This optical behavior was analyzed in an ensemble-averaged fashion to gain general insight into the mixture composition (see above). However, partly because heterogeneous broadening effects are removed, useful and unique information can be gained from single-particle studies, such as the exact distribution of the plasmon resonance energy and width.

As shown in Figure 4A, the optical response of RD supported on no. 2 glass coverslips consists of one main resonance, while that of BPs contains a dominant dipolar mode at low energy and a weak peak at higher energy, which is likely quadrupolar in origin.[38] Figure 4B shows that the distribution of the dominant dipolar plasmon resonance in the RD sample is centered at 569 nm (N = 81); its narrow standard deviation of 7 nm highlights the small size/shape distribution in this sorted fraction. Being considerably larger and more anisotropic, the BPs display a dipolar plasmon resonance redshifted in relationship to that of the RD. Fractions 24 and 27 have an average LSPR maximum (standard deviation) of 617(6) nm (N = 81) and 620(6) nm (N = 76), respectively (see complete data in the Supporting Information, Table S4). The LSPR maxima observed on glass were at lower energy than in solution (see Figure S3), as expected from the different dielectric environment. A t-test reveals that the two populations are statistically different at the 95% confidence level (probability of a type 1 error p = 0.0007), further emphasizing the capability of the separation method and its prospective use for sorting heterogeneous reaction mixtures.

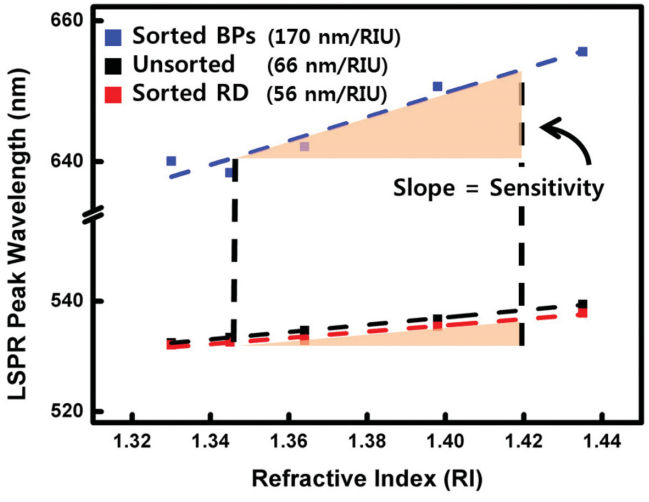

Figure 3. Refractive index dependence of the dipolar LSPR resonance energy for the unsorted, sorted RD, and sorted BP AuNPs. The squares are the experimental data, and the dashed lines are linear fits. The sorted BPs show a sensitivity of 170 nm/RIU, which is 2.5 times that of the as-synthesized, unsorted mixture.

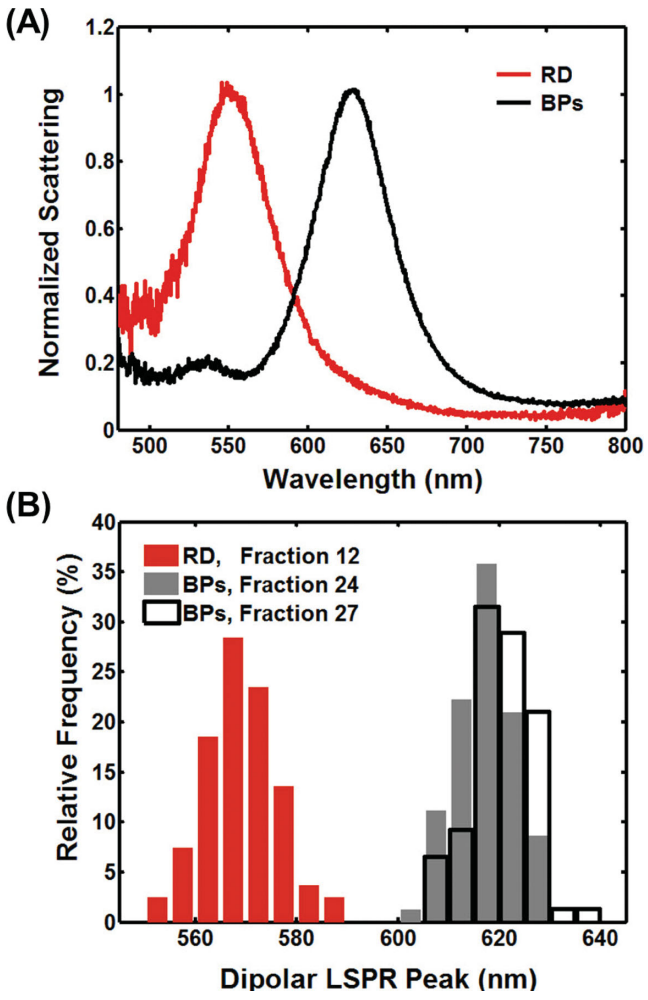

Figure 4. A) Single-particle LSPR spectra. B) Distribution of dipolar plasmon resonance in the sorted RD and BP samples.

Single-particle studies also offer unique insight into the plasmon decay behavior through linewidth analysis. The BP samples on glass (Fractions 24 and 27) do not have statistically different FWHM distributions ($p = 0.09$), even though this would be expected for samples with a dissimilar energy distribution. In the current results, this difference is not realized owing to the larger variance of the FWHM and the small gap in energy between the two samples (yielding even smaller gaps in FWHM). In contrast, a statistically significant difference in the plasmon decay exists between the BP and RD samples, as well as between those on glass and carbon substrates owing to the lossy character of carbon films (see Supporting Information, Figure S4). The small size range for the BPs prevented the acquisition of statistically relevant energy/FWHM, size/energy, and size/FWHM relationships (single-particle correlated LSPR/TEM (transmission electron miscroscopy) measurements in the Supporting Information, Figure S5). The RD, however, displayed a strong LSPR energy/FWHM correlation ($p < 0.001$) in which, as expected, the FWHM increases as the resonance energy redshifts (see Supporting Information, Figure S6).

In conclusion, we have developed a centrifugal route for separating small (edge length < 100 nm) {110}-faceted gold nanostructures, namely RD and triangular BPs, which form simultaneously during synthesis and cannot be separated by means of conventional filtration methods. Centrifugation in a shallow density gradient allows the enrichment of the original minority BP species, which enables a 2.5 times increase in refractive index sensitivity compared to the as-synthesized, unsorted mixture. Furthermore, the sorted BPs and RD have been studied at the single-particle level using dark-field microscopy, which provides further insight into the differences in plasmonic behavior between closely spaced fractions. We anticipate that, in addition to providing a scalable pathway for isolating plasmonically desirable sub-100 nm BP gold nanoparticles, the density gradient centrifugation approach can improve the monodispersity of other metal nanoparticles, leading to concomitant improvements in plasmonic properties and applications.

Experimental Section

Experimental details of the synthesis of {110}-faceted RD and triangular BPs are provided in the Supporting Information. Following synthesis, 4 mL of faceted AuNPs were concentrated ~20-fold by centrifuging at 10 krpm for 10 min to fully sediment the AuNPs to the bottom of the centrifuge tube, and then 3.6 mL of the supernatant was decanted and replaced with deionized water. After this process had been repeated twice, the supernatant was replaced with an aqueous 0.04 M CTAC solution to make 200 µL of the concentrated solution, which was then sonicated for 10 min, ultimately resulting in a well-dispersed AuNP solution. The concentrated, dark pink colored solution was loaded on the top of the density gradient medium in an Ultra-Clear centrifuge tube (Beckman Coulter), which had 1 mL of 60% w/v iodixanol solution (1.32 g cm^{-3}) as an underlayer and 10 mL of a linear density gradient of 30%–40% w/v iodixanol solution (1.16–1.21 g cm^{-3}) above it. All solutions also contained 0.04 M CTAC to inhibit aggregation during centrifugation.

Supporting Information

Supporting Information is available from the Wiley Online Library or from the author.

Acknowledgements

This work was supported by the National Science Foundation through the Northwestern University Materials Research Science and Engineering Center (NU-MRSEC, NSF DMR-1121262). This research made use of the NUANCE Center at Northwestern University, which is supported by NSF-NSEC, NSF-MRSEC, Keck Foundation, and the State of Illinois.

Received: March 21, 2013
Revised: May 18, 2013
Published online:

[1] A. D. McFarland, R. P. Van Duyne, *Nano Lett.* **2003**, *3*, 1057.
[2] R. Jin, Y. Cao, C. A. Mirkin, K. L. Kelly, G. C. Schatz, J. G. Zheng, *Science* **2001**, *294*, 1901.
[3] C. L. Haynes, R. P. Van Duyne, *J. Phys. Chem. B* **2001**, *105*, 5599.
[4] T. R. Jensen, M. D. Malinsky, C. L. Haynes, R. P. Van Duyne, *J. Phys. Chem. B* **2000**, *104*, 10549.

[5] J. N. Anker, W. P. Hall, O. Lyandres, N. C. Shah, J. Zhao, R. P. Van Duyne, *Nat. Mater.* **2008**, *7*, 442.
[6] K. M. Mayer, J. H. Hafner, *Chem. Rev.* **2011**, *111*, 3828.
[7] N. L. Rosi, C. A. Mirkin, *Chem. Rev.* **2005**, *105*, 1547.
[8] J. A. Dionne, L. A. Sweatlock, H. A. Atwater, A. Polman, *Phys. Rev. B* **2006**, *73*, 035407.
[9] L. B. Sagle, L. Ruvuna, J. M. Bingham, C. Liu, P. S. Cremer, R. P. Van Duyne, *J. Am. Chem. Soc.* **2012**, *134*, 15832.
[10] P. L. Stiles, J. A. Dieringer, N. C. Shah, R. P. Van Duyne, *Annu. Rev. Anal. Chem.* **2008**, *1*, 601.
[11] L. Brus, *Acc. Chem. Res.* **2008**, *41*, 1742.
[12] A. J. Haes, L. Chang, W. L. Klein, R. P. Van Duyne, *J. Am. Chem. Soc.* **2005**, *127*, 2264.
[13] G.-T. Wei, F.-K. Liu, C. R. C. Wang, *Anal. Chem.* **1999**, *71*, 2085.
[14] N. Surugau, P. L. Urban, *J. Sep. Sci.* **2009**, *32*, 1889.
[15] V. Sharma, K. Park, M. Srinivasarao, *Proc. Natl. Acad. Sci. USA* **2009**, *106*, 4981.
[16] G. Chen, Y. Wang, L. H. Tan, M. Yang, L. S. Tan, Y. Chen, H. Chen, *J. Am. Chem. Soc.* **2009**, *131*, 4218.
[17] T. P. Tyler, P. A. Lin, Y. Tian, H.-J. Gao, X. P. A. Gao, R. M. Sankaran, M. C. Hersam, *J. Phys. Chem. Lett.* **2012**, *3*, 1484.
[18] T. P. Tyler, A.-I. Henry, R. P. Van Duyne, M. C. Hersam, *J. Phys. Chem. Lett.* **2011**, *2*, 218.
[19] O. Akbulut, C. F. Mace, A. W. Martinez, A. A. Kumar, Z. Nie, M. R. Patton, G. M. Whitesides, *Nano Lett.* **2012**, *12*, 4060.
[20] R. C. Jin, Y. C. Cao, E. C. Hao, G. S. Métraux, G. C. Schatz, C. A. Mirkin, *Nature* **2003**, *425*, 487.
[21] J. J. Mock, M. Barbic, D. R. Smith, D. A. Schultz, S. Schultz, *J. Chem. Phys.* **2002**, *116*, 6755.
[22] M. L. Personick, M. R. Langille, J. Zhang, C. A. Mirkin, *Nano Lett.* **2011**, *11*, 3394.
[23] B. J. Wiley, S. H. Im, Z.-Y. Li, J. McLellan, A. Siekkinen, Y. Xia, *J. Phys. Chem. B* **2006**, *110*, 15666.
[24] T. K. Sau, C. J. Murphy, *J. Am. Chem. Soc.* **2004**, *126*, 8648.
[25] M. Z. Liu, P. Guyot-Sionnest, *J. Phys. Chem. B* **2005**, *109*, 22192.
[26] Y. Xia, Y. Xiong, B. Lim, S. E. Skrabalak, *Angew. Chem. Int. Ed.* **2009**, *48*, 60.
[27] S. J. Hurst, E. K. Payne, L. Qin, C. A. Mirkin, *Angew. Chem. Int. Ed.* **2006**, *45*, 2672.
[28] J. Zhang, M. R. Langille, M. L. Personick, K. Zhang, S. Li, C. A. Mirkin, *J. Am. Chem. Soc.* **2010**, *132*, 14012.
[29] M. R. Langille, M. L. Personick, J. Zhang, C. A. Mirkin, *J. Am. Chem. Soc.* **2012**, *134*, 14542.
[30] P. Mulvaney, *Langmuir* **1996**, *12*, 788.
[31] A.-I. Henry, J. M. Bingham, E. Ringe, L. D. Marks, G. C. Schatz, R. P. Van Duyne, *J. Phys. Chem. C* **2011**, *115*, 9291.
[32] X. Xia, J. Zeng, B. McDearmon, Y. Zheng, Q. Li, Y. Xia, *Angew. Chem. Int. Ed.* **2011**, *50*, 12542.
[33] E. Ringe, J. M. McMahon, K. Sohn, C. Cobley, Y. Xia, J. Huang, G. C. Schatz, L. D. Marks, R. P. Van Duyne, *J. Phys. Chem. C* **2010**, *114*, 12511.
[34] S. Lee, K. M. Mayer, J. H. Hafner, *Anal. Chem.* **2009**, *81*, 4450.
[35] J. Burgin, M. Z. Liu, P. Guyot-Sionnest, *J. Phys. Chem. C* **2008**, *112*, 19279.
[36] M. J. Guffey, R. L. Miller, S. K. Gray, N. F. Scherer, *Nano Lett.* **2011**, *11*, 4058.
[37] A. Lombardi, M. Loumaigne, A. Crut, P. Maioli, N. Del Fatti, F. Vallée, M. Spuch-Calvar, J. Burgin, J. Majimel, M. Tréguer-Delapierre, *Langmuir* **2012**, *28*, 9027.
[38] M. L. Personick, M. R. Langille, J. Zhang, N. Harris, G. C. Schatz, C. A. Mirkin, *J. Am. Chem. Soc.* **2011**, *133*, 6170.
[39] H. Chen, X. Kou, Z. Yang, W. Ni, J. Wang, *Langmuir* **2008**, *24*, 5233.
[40] Z. Guo, Y. Wan, M. Wang, L. Xu, X. Lu, G. Yang, K. Fang, N. Gu, *Colloids Surf. A* **2012**, *414*, 492.
[41] J. B. Hubbard, J. F. Douglas, *Phys. Rev. E* **1993**, *47*, R2983.
[42] E. Ringe, M. R. Langille, K. Sohn, J. Zhang, J. Huang, C. A. Mirkin, R. P. Van Duyne, L. D. Marks, *J. Phys. Chem. Lett.* **2012**, *3*, 1479.
[43] E. Ringe, J. Zhang, M. R. Langille, C. A. Mirkin, L. D. Marks, R. P. Van Duyne, *Nanotechnology* **2012**, *23*, 444005.